




Cite this: *RSC Adv.*, 2021, 11, 16435

# Complex oscillations in the Belousov–Zhabotinsky batch reaction with methylmalonic acid and manganese(II)

Glen A. Frerichs <sup>\*a</sup> and Desmond Yengi <sup>b</sup>

The Belousov–Zhabotinsky (BZ) oscillating chemical reaction involves the oxidation of an organic compound by the bromate ion in the presence of a metal ion catalyst such as cerium(IV), manganese(II), or ferroin. Simple periodic oscillations are generally obtained for the BZ reaction in a batch (closed) system. However, complex oscillations have been observed for the BZ reaction in batch with malonic acid and either cerium or ferroin ions as the catalyst. We report here that fascinating complex oscillations in the potential of a Pt electrode have been found in the batch BZ reaction with methylmalonic acid (MeMA) and manganese(II). Relatively high initial concentrations of  $\text{NaBrO}_3$  and MeMA are required, and the  $[\text{NaBrO}_3]_0/[\text{MeMA}]_0$  ratio is the main factor determining the type of oscillations obtained. Other relevant factors are  $[\text{NaBr}]_0$ ,  $[\text{MnSO}_4]_0$ ,  $[\text{H}_2\text{SO}_4]_0$  or  $[\text{NaOH}]_0$ , temperature, and stirring rate. Complex phenomena observed include mixed mode oscillations, birhythmicity, quasiperiodicity, bursting, and possible chaos. A mechanism is proposed involving the reversible formation of a manganese(III) complex with bromomethylmalonic acid followed by two-electron oxidation to methyltartronic acid and  $\text{Mn}^{2+}$ .

Received 4th March 2021

Accepted 21st April 2021

DOI: 10.1039/d1ra01734a

rsc.li/rsc-advances

## Introduction

The oscillation patterns exhibited in the rhythmic beating of cardiac pacemaker cells, the central pattern generators that control rhythmic actions, and the bursting patterns found in various types of neurons due to changing membrane potential are similar to those observed under certain conditions in the Belousov–Zhabotinsky (BZ) reaction system. In the well-studied BZ oscillating chemical reaction an organic compound is oxidized by the bromate ion in the presence of a metal ion catalyst such as cerium(IV), manganese(II), ruthenium(II), or ferroin. The classical BZ system consists of malonic acid (MA),  $\text{BrO}_3^-$ , and  $\text{Ce(IV)}$  in  $\text{H}_2\text{SO}_4$ .<sup>1</sup> Chemical oscillations have been observed for the BZ reaction both in a closed (batch) reactor and in a continuous-flow stirred tank reactor (CSTR). Among the organic substrates found to give oscillations with the BZ system is methylmalonic acid (MeMA).

Most commonly, the BZ reaction in batch gives simple periodic oscillations in absorbance at a fixed wavelength and/or in potential of a Pt or specific-ion electrode *versus* a reference electrode. However, in a few BZ systems with MA in batch, complex oscillations have been observed. Ruoff<sup>2</sup> reported chaotic behavior in the BZ reaction catalyzed by cerium ion.

Wang, Sorensen and Hynne<sup>3</sup> found period doubling, intermittency, mixed mode and quasiperiodic oscillations in the BZ reaction also with cerium ion. Kawczynski *et al.*<sup>4,5</sup> obtained mixed mode oscillations in the BZ reaction catalyzed by ferroin. Johnson, Scott and Thompson<sup>6</sup> confirmed the complex oscillations of Wang *et al.* and modeled this behavior in the cerium-catalyzed BZ reaction. Experimental and numerical evidence for complex oscillations in the BZ reaction catalyzed by cerium in batch was reported subsequently by Kolar-Anic *et al.*<sup>7</sup> and Blagojevic *et al.*<sup>8</sup>

Manganese(II)-catalyzed BZ systems have been less studied than those catalyzed by cerium(IV) or ferroin. Hansen and Ruoff<sup>9</sup> used NMR to observe oscillations in a closed BZ system using MeMA and catalyzed by Mn(II). Subsequently, Jwo *et al.*<sup>10</sup> reported on a thorough study of the Mn(II)-catalyzed BZ reaction in batch with MeMA as well as with other related acids of MA. The reaction was followed potentiometrically with a bromide ion selective electrode and periodic oscillations were obtained. In both of these studies using Mn(II) as catalyst only simple periodic oscillations were obtained.

Recently, Frerichs *et al.*<sup>11</sup> reported the surprising result that the closed BZ system containing  $\text{BrO}_3^-$ , MA, and Mn(II) gave significant pH oscillations under a variety of conditions. The conclusion was that the pH oscillations were due primarily to the reversible formation of a manganese(III) complex with bromomalonic acid. Because of the close similarity in their structures, it was decided to search for pH oscillations with the BZ reaction using MeMA in place of MA. Although significant pH

<sup>a</sup>Department of Chemistry, Westminster College, 501 Westminster Ave, Fulton, MO, 65251, USA. E-mail: glen.frerichs@westminster-mo.edu; Tel: +1-573-310-4108

<sup>b</sup>College of Arts and Sciences, Ohio Valley University, 1 Campus View Drive, Vienna, WV, 26105, USA



oscillations were not found, a variety of fascinating complex oscillations, to our knowledge never reported before in this system, were observed.

Our goal in this study is to uncover the wide range of oscillation patterns exhibited by the Mn(II)-catalyzed BZ reaction with MeMA as the organic substrate in a batch reactor. The oscillation patterns found include simple periodic oscillations, mixed mode oscillations (MMO), birhythmicity (BI), bursting (BR), quasiperiodicity (Q), and possible chaotic oscillations. We first describe the experimental procedure used, present the results in relation to how different conditions of reaction mixture composition, temperature, and stirring rate affect the oscillation patterns, then discuss observed oscillations in the context of a possible reaction mechanism for the BZ system, and finally provide a conclusion.

## Experimental section

Experiments were carried out in a glass reactor covered by a reactor cap and having a total solution volume of about 50 mL. The cap had a small opening covered by ParaFilm having a very small perforation. A Pt electrode and a combination pH electrode, each with a Ag/AgCl reference electrode, were inserted in the reactor cap. Both potential and pH were recorded concurrently using a Servogor 124 chart recorder. Stirring was done at various rates from 308 to 886 rpm using a Teflon-coated stir bar and either a Fisher Scientific or Heidolph Hei-Standard stirrer. Runs were carried out at room temperature ( $21 \pm 1$ ) °C, as well as at 25, 30, and 40 °C using a constant-temperature circulator. The reagents NaBrO<sub>3</sub> (Fisher), MeMA (TCI), NaBr (Fisher) and MnSO<sub>4</sub>·H<sub>2</sub>O (Fisher) were ACS-certified. Ultrapure water was bubbled with N<sub>2</sub> for about an hour before use.

Initially, the procedure for experiments was to add the solid reagents directly to the water in the reactor. Later, some runs

were done using pre-dissolved NaBrO<sub>3</sub>. Eventually, the procedure involved pre-dissolving both NaBrO<sub>3</sub> and MeMA before adding MnSO<sub>4</sub>·H<sub>2</sub>O and NaBr in that order. In most runs, H<sub>2</sub>SO<sub>4</sub> was used and was added before the other reagents. A few experiments were done using NaOH, and some were carried out without either acid or base. Since the reaction vessel used was a CSTR reactor with closed ports, a few experiments were carried out at room temperature using a 100 mL beaker and comparable results were obtained.

## Results

Early experiments involved using conditions somewhat comparable to those used by Jwo *et al.*, except [H<sub>2</sub>SO<sub>4</sub>]<sub>0</sub> was lower in our study. Also, our experiments were carried out at room temperature with NaBrO<sub>3</sub>, MeMA, and MnSO<sub>4</sub> being added as solids directly to an H<sub>2</sub>SO<sub>4</sub> solution in the reactor. Not having had success in obtaining oscillations under these conditions, it was decided to include NaBr as a solid reagent. Large oscillations in potential were obtained using [NaBrO<sub>3</sub>]<sub>0</sub> = 0.100–0.200 M, [MeMA]<sub>0</sub> = 0.120 M, [NaBr]<sub>0</sub> = 0.0100–0.0200 M, [MnSO<sub>4</sub>]<sub>0</sub> = 0.00600 M, and [H<sub>2</sub>SO<sub>4</sub>]<sub>0</sub> = 0.150–0.300 M. A typical result is shown in Fig. 1(a). Immediately after addition of all reactants the solution color was dark orange. During the induction period, the color went through the transition to lighter orange, yellow, and then nearly colorless before oscillations began. As each peak was formed, the solution color became pink to light tan.

In between oscillations, the solution again became nearly colorless, suggesting a transition from Mn(III) to Mn(II) ions. Oscillations were periodic, but not symmetric, as typically a “shoulder” appeared as the peak returned to the baseline. These oscillations continued for an extended period of time, sometimes for hours.

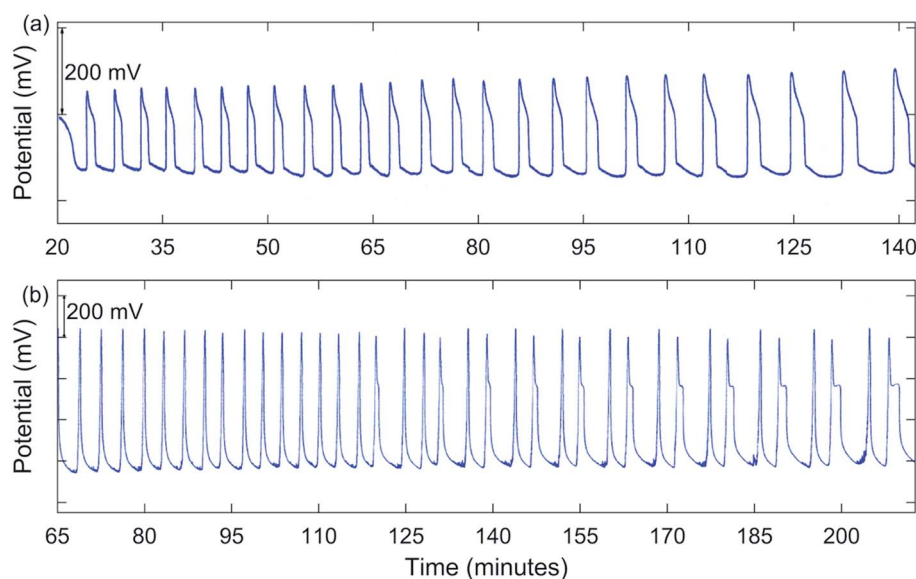


Fig. 1 Measured Pt potential for the BZ-MeMA system in batch: (a) simple periodic oscillations at 25 °C. [NaBrO<sub>3</sub>]<sub>0</sub> = 0.200 M; [MeMA]<sub>0</sub> = 0.120 M; [NaBr]<sub>0</sub> = 0.0200 M; [MnSO<sub>4</sub>]<sub>0</sub> = 0.00600 M; [H<sub>2</sub>SO<sub>4</sub>]<sub>0</sub> = 0.150 M.; (b) mixed mode oscillations [(3<sup>1</sup>(2<sup>1</sup>))<sub>9</sub>...] at room temperature. [NaBrO<sub>3</sub>]<sub>0</sub> = 1.00 M; [MeMA]<sub>0</sub> = 0.571 M; [NaBr]<sub>0</sub> = 0.100 M; [MnSO<sub>4</sub>]<sub>0</sub> = 0.0100 M; [H<sub>2</sub>SO<sub>4</sub>]<sub>0</sub> = 0.010 M.



Since much higher  $[\text{NaBrO}_3]_0$  and lower  $[\text{H}_2\text{SO}_4]_0$  were used in our investigation with MA, it was decided to follow the same approach in the present study with MeMA. With  $[\text{NaBrO}_3]_0 = 0.800 \text{ M}$ ,  $[\text{MeMA}]_0 = 0.250\text{--}0.500 \text{ M}$ ,  $[\text{NaBr}]_0 = 0.0800 \text{ M}$ ,  $[\text{MnSO}_4]_0 = 0.00600\text{--}0.00750 \text{ M}$ , and  $[\text{H}_2\text{SO}_4]_0 = 0.0150\text{--}0.0375 \text{ M}$ , periodic oscillations occurred as in the earlier experiments, but in this case a brown color was observed during formation of a peak and an amber color in between peaks.

A significant change in the nature of the oscillations occurred when  $[\text{NaBrO}_3]_0$  was increased to  $1.00 \text{ M}$ . Runs were carried out with  $[\text{MeMA}]_0 = 0.400\text{--}1.25 \text{ M}$ ,  $[\text{NaBr}]_0 = 0.100 \text{ M}$ ,  $[\text{MnSO}_4]_0 = 0.0100 \text{ M}$ , and  $[\text{H}_2\text{SO}_4]_0 = 0.0100 \text{ M}$ . Under these conditions complex oscillations were observed for the first time. These were of the mixed mode types  $2^1$  and  $3^1$ , using the notation  $L^S$  where  $L$  is the number of large-amplitude oscillations followed by  $S$  small-amplitude oscillations. One such result is shown in Fig. 1(b).

Subsequently, a series of runs was done with varying  $[\text{MeMA}]_0$ , not only for  $1.00 \text{ M NaBrO}_3$ , but also for  $1.60 \text{ M}$  and

$2.00 \text{ M NaBrO}_3$ . An overall summary of the results is given in Table 1. Reactant concentrations used for  $\text{NaBr}$ ,  $\text{MnSO}_4$ , and  $\text{H}_2\text{SO}_4$  are given in the table. A variety of mixed mode oscillations (MMO) was obtained, ranging from  $2^1$  to  $10^2$ .

Perhaps the principal conclusions to be drawn from Table 1 are that the  $[\text{NaBrO}_3]_0/[\text{MeMA}]_0$  ratio is the main determinant of whether complex oscillations are obtained, and of what type. For runs done with  $1.00 \text{ M NaBrO}_3$ , MMO were observed over a reactant ratio range of  $2.50 : 1$  to  $1.00 : 1$ . With  $1.60 \text{ M NaBrO}_3$ , MMO were found over a range of  $4.44 : 1$  to  $1.25 : 1$ , and with  $2.00 \text{ M NaBrO}_3$  the reactant ratio range giving complex oscillations was  $3.70 : 1$  to  $1.00 : 1$ . Also, the greater the initial concentration of  $\text{NaBrO}_3$  the more complex the oscillations tended to be. Further, for a given  $[\text{NaBrO}_3]_0$  the complexity of oscillations generally increased with decreasing  $[\text{NaBrO}_3]_0/[\text{MeMA}]_0$  ratio (*i.e.*, with increasing  $[\text{MeMA}]_0$ ). Finally, for a given  $[\text{NaBrO}_3]_0$  both the cap times and induction times tended to decrease with decreasing  $[\text{NaBrO}_3]_0/[\text{MeMA}]_0$  ratio. The “cap” refers to the broad maximum that generally occurs during

Table 1 Dependence of oscillations on  $[\text{NaBrO}_3]_0/[\text{MeMA}]_0$  ratio

Ratio	Cap time (min)	Ind. time (min)	Type of oscillations
<b>Initial concentrations: 1.00 M NaBrO<sub>3</sub>; 0.100 M NaBr; 0.0100 M MnSO<sub>4</sub>; 0.0100 M H<sub>2</sub>SO<sub>4</sub>; room temp.</b>			
2.50 : 1	19	45	$(2^1)_5 2^0$
2.00 : 1	17.5	47	Simple periodic oscillations
1.75 : 1	12	31	$3^1(2^1)_9 \dots$
1.50 : 1	9	23	$(3^1)_5(2^1)_3(3^1 2^1)_2(2^1)_2 2^0$
1.33 : 1	8	19	$(2^1)_{11} \dots$
1.00 : 1	5	15	$(3^1)_{12} \dots$
0.80 : 1	4.5	10.5	Simple periodic oscillations
<b>Initial concentrations: 1.60 M NaBrO<sub>3</sub>; 0.160 M NaBr; 0.0100 M MnSO<sub>4</sub>; 0.0188 M H<sub>2</sub>SO<sub>4</sub>; room temp.</b>			
4.44 : 1	37.5	56	$(2^1)_2 1^0$
4.20 : 1	35.4	53	$(2^1)_3 2^0$
4.00 : 1	28	42	$(2^1)_5 2^0$
3.60 : 1	25.5	38	$(2^1)_6(1^1)_5 1^0$
3.20 : 1	18.5	33	$(2^1)_{14} 2^0$
2.80 : 1	16.9	28.5	$2^1(3^1)_3(2^1)_{11}(2^1)_2 2^n$
2.50 : 1	14.1	22	$(2^1)_{13} 2^n$
2.22 : 1	12.5	22	$3^1(2^1)_{11} 2^2 2^3 2^n$
2.00 : 1	12.4	22.8	$(2^1)_{16}(2^1)_2 2^3 2^4 2^n$
1.75 : 1	11.5	18.5	$3^1 2^1(3^1)_2(2^1)_2(3^1)_2 2^1 3^1(2^1)_4 3^1(2^1)_3 2^1$
1.50 : 1	8.4	12.4	$(2^1)_{13} 3^2 2^2 3^2 3^3 3^4 3^5 3^n$
1.25 : 1	7.2	12	$(3^1)_6 2^1(3^1)_3 3^2(3^1)_2 3^4 3^6 3^n$
1.00 : 1	5.6	9	Simple periodic oscillations
<b>Initial concentrations: 2.00 M NaBrO<sub>3</sub>; 0.200 M NaBr; 0.0150 M MnSO<sub>4</sub>; 0.0100 M H<sub>2</sub>SO<sub>4</sub>; room temp.</b>			
3.70 : 1	23.5	40	$(3^1)_2 3^0$
3.50 : 1	22	35	$3^1 4^1 4^2 3^n$
3.20 : 1	18	33	$(3^1)_6 2^1 2^n$
2.80 : 1	14	22	$2^2 4^1(3^1)_6 2^1 3^1 3^2 3^n$
2.50 : 1	12	19	$(3^1)_4 3^2 3^3 3^5 3^n$
2.25 : 1	12	19	$(3^1)_6 3^2 3^3 3^4 3^n$
2.00 : 1	9	14	$(3^1)_7(3^1)_2 3^3 3^4 3^7 3^n$
1.50 : 1	7.5	11.5	$4^1 5^1(4^1)_9 \dots 4^n$
1.25 : 1	5.2	8	$(5^1)_8 5^5 5^n$
1.12 : 1	4	6.8	$7^1 6^1 6^2(6^n)_3$
1.00 : 1	4.4	6.8	$10^2 9^3 8^n$
0.80 : 1	3.4	5.1	Shifting clusters of peaks



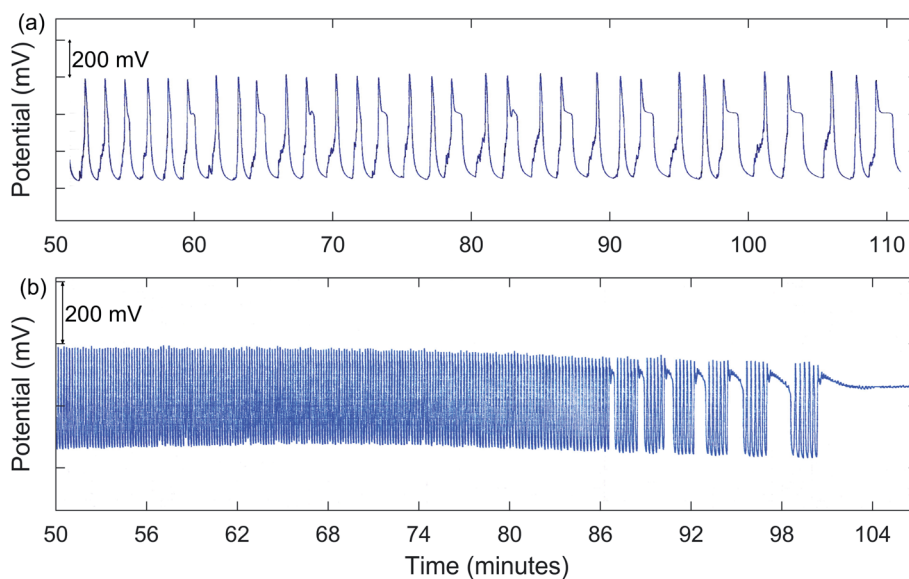


Fig. 2 Measured Pt potential for the BZ-MeMA system in batch at room temperature: (a) chaotic oscillations  $[3^1 2^1 (3^1)_2 (2^1)_2 (3^1)_2 2^1 3^1 \dots]$ .  $[\text{NaBrO}_3]_0 = 1.00 \text{ M}$ ;  $[\text{MeMA}]_0 = 0.667 \text{ M}$ ;  $[\text{NaBr}]_0 = 0.100 \text{ M}$ ;  $[\text{MnSO}_4]_0 = 0.0100 \text{ M}$ ;  $[\text{H}_2\text{SO}_4]_0 = 0.010 \text{ M}$ ; (b) bursting oscillations  $[7^1 (6^1)_5]$ .  $[\text{NaBrO}_3]_0 = 2.00 \text{ M}$ ;  $[\text{MeMA}]_0 = 1.79 \text{ M}$ ;  $[\text{NaBr}]_0 = 0.200 \text{ M}$ ;  $[\text{MnSO}_4]_0 = 0.0150 \text{ M}$ ;  $[\text{H}_2\text{SO}_4]_0 = 0.010 \text{ M}$ .

the early part of the run with the transition from increasing to decreasing potential. This precedes a more gradual decrease in potential that leads to the onset of oscillations.

In addition to simple MMO, other types of complex oscillations are suggested by the results summarized in Table 1. Numerous experiments demonstrated possible chaos. A good example is for 1.00 M  $\text{NaBrO}_3$  with a  $[\text{NaBrO}_3]_0/[\text{MeMA}]_0$  ratio of 1.50 : 1, as shown in Fig. 2(a). Also, bursting appears to be present for 2.00 M  $\text{NaBrO}_3$ , especially at values of  $[\text{NaBrO}_3]_0/[\text{MeMA}]_0$  from 1.50 : 1 to 1.00 : 1. This phenomenon, which occurs when periods of quiescent behavior alternate with periods of relatively fast large-amplitude oscillations, is illustrated in Fig. 2(b).

Using the procedure described above, with  $[\text{NaBrO}_3]_0 = 1.60 \text{ M}$  and  $[\text{MeMA}]_0 = 0.500 \text{ M}$ , the dependence of oscillations on temperature,  $[\text{NaBr}]_0$ ,  $[\text{MnSO}_4]_0$ , and presence of acid or base was investigated. The results are summarized in Table 2. Regarding the effect of temperature, similar MMO were observed at room temperature, at 20 °C, and at 25 °C, the main difference being the number of  $2^1$  oscillations. Not surprisingly, the cap time, induction time, and period of oscillations all decreased with increasing temperature. As to the dependence of oscillations on  $[\text{NaBr}]_0$ , good MMO were found with 0.160 M and 0.240 M  $\text{NaBr}$ , but the former had many more  $2^1$  oscillations. Interestingly, both the cap time and induction time were reduced as  $[\text{NaBr}]_0$  was lowered. Also, similar MMO were obtained with 0.0100 M and 0.0120 M  $\text{MnSO}_4$ , although the former gave significantly more  $2^1$  oscillations. Regarding the impact of acid or base, good MMO were obtained with 0.0188 M  $\text{H}_2\text{SO}_4$ , with 0.010 M and 0.020 M  $\text{NaOH}$ , as well as with no acid or base added. One difference was that  $2^1$  oscillations were found with  $\text{H}_2\text{SO}_4$ , whereas  $3^1$  oscillations were the main type observed with  $\text{NaOH}$  or with no added acid or base.

Because the dissolution of  $\text{NaBrO}_3$  in water is an endothermic process, and also to be sure the solid is completely dissolved before any reaction begins, it was decided to pre-dissolve  $\text{NaBrO}_3$  before adding it to the reactor. Also, the initial reaction of  $\text{NaBrO}_3$  with  $\text{NaBr}$  is quite exothermic. Thus, in order to eliminate any possible temperature effect, a constant-temperature circulator was used to maintain the reactor at 25 °C. A number of experiments were done using this procedure, including many runs with the same reactant concentrations as used previously. Although solid MeMA generally dissolved very readily after being added to the reactor, eventually it was decided to pre-dissolve this reactant as well. All subsequent experiments were done using the above method.

Since Ruoff and Schwitters<sup>12</sup> had reported a stirring effect on the number and shape of oscillations in their study of the closed BZ system with MeMA and  $\text{Ce(IV)}$ , it was thought important to investigate this effect also in the present system. Previously, all runs were carried out at the rather slow stirring rate of 308 rpm. To determine the effect of stirring rate, the present system was explored over a wide range from 308 to 886 rpm. Several previously used sets of concentrations were studied. The results are summarized in Table 3. It is clear that stirring rate can have a significant effect on the type of complex oscillatory behavior exhibited.

In addition to MMO, birhythmicity (BI), bursting (BR), and quasiperiodicity (Q), along with possible chaos, were observed. An example of a run giving MMO and BI is shown in Fig. 3(a), and one showing a transition from MMO to Q and BR is given in Fig. 3(b). In the case of birhythmicity, a lower oscillatory state first appeared with peak amplitudes in the 1–40 mV range. Later in the run, there was a very large increase in potential to a higher oscillatory state and these peaks typically had amplitudes of 200–300 mV. Quasiperiodicity involves the appearance



**Table 2** Dependence of oscillations on temperature,  $[\text{NaBr}]_0$ ,  $[\text{MnSO}_4]_0$ , and  $[\text{H}_2\text{SO}_4]_0$  or  $[\text{NaOH}]_0$ 

Initial Conditions: 1.60 M $\text{NaBrO}_3$ ; 0.500 M MeMA; 0.160 M NaBr; 0.0100 M $\text{MnSO}_4$ ; 0.0188 M $\text{H}_2\text{SO}_4$				
(°C) temperature	Cap time (min)	Ind. time (min)	Period (min)	Type of oscillations
Room temp.	18.5	33	5–6	$(2^1)_{14}2^0$
20	20	34	8.5–12.4	$(2^1)_{11}2^0$
25	14	25	5.4–7	$(2^1)_{13}2^0$
30	9.6	14.8	1.8–3.2	$(1^1)_{13}1^n$
40	3.5	5.2	1.8–3.2	$(1^1)_{61}1^n$
Initial conditions: 1.60 M $\text{NaBrO}_3$ ; 0.500 M MeMA; 0.0100 M $\text{MnSO}_4$ ; 0.0188 M $\text{H}_2\text{SO}_4$ ; room temp.				
$[\text{NaBr}]_0$ , M	Cap time (min)	Ind. time (min)	Period (min)	Type of oscillations
0.280	38.4	66.6	—	$1^02^12_0$
0.240	31.4	50.6	6–7.2	$1^1(2^1)_62^0$
0.160	18.5	33	5–6	$(2^1)_{14}2^0$
0.0800	14	19.2	3.8–5.4	$(2^2)_2(1^1)_{15}1^21^41^71^n$
0.0400	9	12.4	3–5.6	$2^1(1^1)_{18}(1^2)_31^31^41^81^n$
None	22.2	24.8	3.6–6.2	$(1^1)_{15}1^31^41^81^n$
Initial conditions: 1.60 M $\text{NaBrO}_3$ ; 0.500 M MeMA; 0.160 M NaBr; 0.0188 M $\text{H}_2\text{SO}_4$ ; room temp.				
$[\text{MnSO}_4]_0$ , M	Cap time (min)	Ind. time (min)	Period (min)	Type of oscillations
0.0240	21.6	33.2	—	$2^n$
0.0150	23.4	34.4	—	$2^12^0$
0.0120	20.6	31.4	6	$(2^1)_72^12^n$
0.0100	18.5	33	5–6	$(2^1)_{14}2^0$
0.00750	22	32.4	3.8–5.4	$2^1(1^1)_{15}1^0$
0.00500	24	36	5–7.2	$2^1$
Initial conditions: 1.60 M $\text{NaBrO}_3$ ; 0.500 M MeMA; 0.160 M NaBr; 0.0100 M $\text{MnSO}_4$ ; 25 °C				
$[\text{H}_2\text{SO}_4]_0$ or $[\text{NaOH}]_0$	Cap time (min)	Ind. time (min)	Period (min)	Type of oscillations
0.0500 M $\text{H}_2\text{SO}_4$	—	—	—	No oscillations
0.0350 M $\text{H}_2\text{SO}_4$	18	21.8	2.6–4.6	$2^1$
0.0188 M $\text{H}_2\text{SO}_4$	14	25	5.4–7	$(2^1)_{13}2^0$
No acid or base	11	38	9.8–10.6	$(5^0)_24^1(3^1)_62^12^0$
0.01 M NaOH	3.8	17.2	3–5.2	$(6^0)_24^0(3^1)_62^0$
0.02 M NaOH	8.2	50.6	12.5–14	$(4^0)_2(4^1)_2(3^1)_33^0$
0.03 M NaOH	18.5	23	3–5.3	$2^1$

of two incommensurate frequencies of oscillations, one much lower than the other. With 1.00 M  $\text{NaBrO}_3$  and 0.667 M MeMA, BI was observed at a stirring rate of 635 rpm or less, while both BI and MMO occurred at 379 and 512 rpm. Interestingly, at 765 rpm period-halving (P-1/2) took place, in which the system switched to a new behavior with half the period of the original oscillations. For the series of runs with 1.60 M  $\text{NaBrO}_3$  and 0.500 M MeMA, MMO were found at all stirring rates, but BI only at 400 rpm or lower.

With 2.00 M  $\text{NaBrO}_3$  and 1.33 M MeMA, BI, Q, and BR were all present except at the highest stir rate (886 rpm), which did not give BI. In the case of 2.00 M  $\text{NaBrO}_3$  and 1.60 M MeMA only the higher oscillatory state was present, with Q and BR being

observed at all stirring rates but MMO only at 635 and 886 rpm. The results in Table 3, including experiments done with 2.00 M  $\text{NaBrO}_3$  and 1.60 M MeMA, suggest that Q and BR are more likely to be observed when  $[\text{NaBrO}_3]_0$  is near the upper limit of concentrations giving complex oscillations, as long as  $[\text{MeMA}]_0$  is sufficiently high. It is to be noted from this table that possible chaos also is more likely to be found under these conditions.

## Discussion

Based on the similarity of the structures of MeMA and MA, it would be reasonable to expect the mechanisms of their reactions in the BZ system to be rather similar. A proposed model is



Table 3 Dependence of oscillations on stirring rate (25 °C)

Code: BI (birhythmicity); BR (bursting); MMO (mixed mode oscillations); Q (quasiperiodicity); P-1/2 (period-halving); NCO (no complex oscillations)	
Stir rate (rpm)	Behavior of system
<b>Initial concentrations: 1.00 M NaBrO<sub>3</sub>; 0.667 M MeMA; 0.100 M NaBr; 0.0100 M MnSO<sub>4</sub>; 0.0100 M H<sub>2</sub>SO<sub>4</sub></b>	
379	Lower state: simple periodic oscillations (2.5–11 mV)
BI,MMO	Higher state: (2 <sup>1</sup> ) <sub>17</sub> 2 <sup>0</sup>
512	Lower state: (3 <sup>1</sup> ) <sub>4</sub> 4 <sup>1</sup> 3 <sup>1</sup> (2 <sup>1</sup> ) <sub>3</sub> (~2 mV)
BI,MMO	Higher state: (2 <sup>1</sup> ) <sub>4</sub> 2 <sup>0</sup>
635	Lower state: simple periodic oscillations (33.5–37.5 mV)
BI	Higher state: simple periodic oscillations
765	Lower state: none
P-1/2	Higher state: (1 <sup>0</sup> 1 <sup>0</sup> ) <sub>3</sub>
886	Lower state: none
NCO	Higher state: simple periodic oscillations
<b>Initial concentrations: 1.60 M NaBrO<sub>3</sub>; 0.500 M MeMA; 0.160 M NaBr; 0.0100 M MnSO<sub>4</sub>; 0.0188 M H<sub>2</sub>SO<sub>4</sub></b>	
0	Lower state: none
MMO	Higher state: 1 <sup>0</sup> (1 <sup>1</sup> ) <sub>3</sub> 1 <sup>0</sup> (1 <sup>1</sup> ) <sub>5</sub> 1 <sup>0</sup> (1 <sup>1</sup> ) <sub>12</sub> 1 <sup>0</sup>
308	Lower state: (2 <sup>1</sup> ) <sub>4</sub> (19–20 mV)
BI,MMO	Higher state: (2 <sup>1</sup> ) <sub>9</sub> 2 <sup>0</sup>
326	Lower state: (3 <sup>1</sup> ) <sub>5</sub> (5–10 mV)
BI,MMO	Higher state: (2 <sup>1</sup> ) <sub>4</sub> 2 <sup>0</sup>
358	Lower state: 3 <sup>1</sup> (11 mV)
BI,MMO	Higher state: (3 <sup>1</sup> ) <sub>4</sub> (2 <sup>1</sup> ) <sub>3</sub> 2 <sup>0</sup>
400	Lower state: (2 <sup>1</sup> ) <sub>7</sub> (6–8 mV)
BI,MMO	Higher state: (2 <sup>1</sup> ) <sub>5</sub> 2 <sup>0</sup>
512	Lower state: 1 <sup>0</sup> 2 <sup>0</sup> 3 <sup>0</sup> (1–2 mV)
MMO	Higher state: (3 <sup>1</sup> ) <sub>6</sub> 2 <sup>1</sup> 2 <sup>0</sup>
635	Lower state: (3 <sup>0</sup> ) <sub>3</sub> (1–2 mV)
MMO	Higher state: 3 <sup>1</sup> 5 <sup>1</sup> (3 <sup>1</sup> ) <sub>4</sub>
765	Lower state: none
MMO	Higher state: (3 <sup>1</sup> ) <sub>4</sub> 2 <sup>1</sup> 2 <sup>0</sup>
886	Lower state: none
MMO	Higher state: 3 <sup>1</sup> 3 <sup>0</sup>
<b>Initial concentrations: 2.00 M NaBrO<sub>3</sub>; 1.33 M MeMA; 0.200 M NaBr; 0.0150 M MnSO<sub>4</sub>; 0.0100 M H<sub>2</sub>SO<sub>4</sub></b>	
308	Lower state: 16 simple periodic oscillations (1–2 mV)
BI,Q,BR	Higher state: (5 <sup>1</sup> ) <sub>2</sub> 3 <sup>1</sup> (4 <sup>1</sup> ) <sub>6</sub> 4 <sup>n</sup>
358	Lower state: simple periodic oscillations (1–2 mV)
BI,Q,BR	Higher state: (4 <sup>1</sup> ) <sub>6</sub> (4 <sup>3</sup> ) <sub>2</sub> 4 <sup>4</sup> 4 <sup>n</sup>
512	Lower state: simple periodic oscillations (20–25 mV)
BI,Q,BR	Higher state: 5 <sup>1</sup> 9 <sup>1</sup> 6 <sup>1</sup> 5 <sup>1</sup> (4 <sup>1</sup> ) <sub>2</sub> 5 <sup>1</sup> (4 <sup>1</sup> ) <sub>2</sub> 4 <sup>0</sup>
635	Lower state: simple periodic oscillations (1.5–2.5 mV)
BI,Q,BR	Higher state: 4 <sup>1</sup> (5 <sup>1</sup> ) <sub>2</sub> 4 <sup>1</sup> (3 <sup>1</sup> 4 <sup>1</sup> ) <sub>3</sub> 3 <sup>1</sup> 3 <sup>0</sup>
765	Lower state: simple periodic oscillations (~2 mV)
BI,Q,BR	Higher state: 10 <sup>1</sup> 8 <sup>1</sup> 5 <sup>1</sup> (6 <sup>1</sup> ) <sub>2</sub> 5 <sup>1</sup> 6 <sup>1</sup> 5 <sup>0</sup>
886	Lower state: none
Q,BR	Higher state: (8 <sup>1</sup> ) <sub>5</sub> 6 <sup>0</sup>
<b>Initial concentrations: 2.00 M NaBrO<sub>3</sub>; 1.60 M MeMA; 0.200 M NaBr; 0.0150 M MnSO<sub>4</sub>; 0.0100 M H<sub>2</sub>SO<sub>4</sub></b>	
358	Lower state: none
Q,BR	Higher state: (6 <sup>1</sup> ) <sub>2</sub> (5 <sup>1</sup> ) <sub>2</sub> (4 <sup>1</sup> ) <sub>4</sub> 4 <sup>0</sup>
512	Lower state: none
Q,BR	Higher state: (5 <sup>1</sup> ) <sub>7</sub> 5 <sup>0</sup>
635	Lower state: none
MMO,Q,BR	Higher state: (2 <sup>1</sup> ) <sub>2</sub> 9 <sup>1</sup> (6 <sup>1</sup> ) <sub>2</sub> (5 <sup>1</sup> ) <sub>3</sub> 4 <sup>0</sup>
765	Lower state: none
Q,BR	Higher state: 7 <sup>1</sup> (4 <sup>1</sup> ) <sub>4</sub> 6 <sup>1</sup> (4 <sup>1</sup> ) <sub>4</sub> 4 <sup>0</sup>
886	Lower state: none
MMO,Q,BR	Higher state: (2 <sup>1</sup> ) <sub>2</sub> 8 <sup>1</sup> 5 <sup>1</sup> 4 <sup>1</sup> (6 <sup>1</sup> ) <sub>4</sub> 7 <sup>1</sup> (5 <sup>1</sup> ) <sub>2</sub> 4 <sup>0</sup>

given in Table 4. As with the model used for the BZ reaction with MA,<sup>11</sup> we include the minimal bromate subsystem which generates Br<sub>2</sub> and Mn<sup>3+</sup>. This is followed by the bromine–

methylmalonic acid subsystem in which MeMA is converted to the enol, which then reacts with Br<sub>2</sub> to produce bromomethylmalonic acid (BrMeMA). Finally, we include the



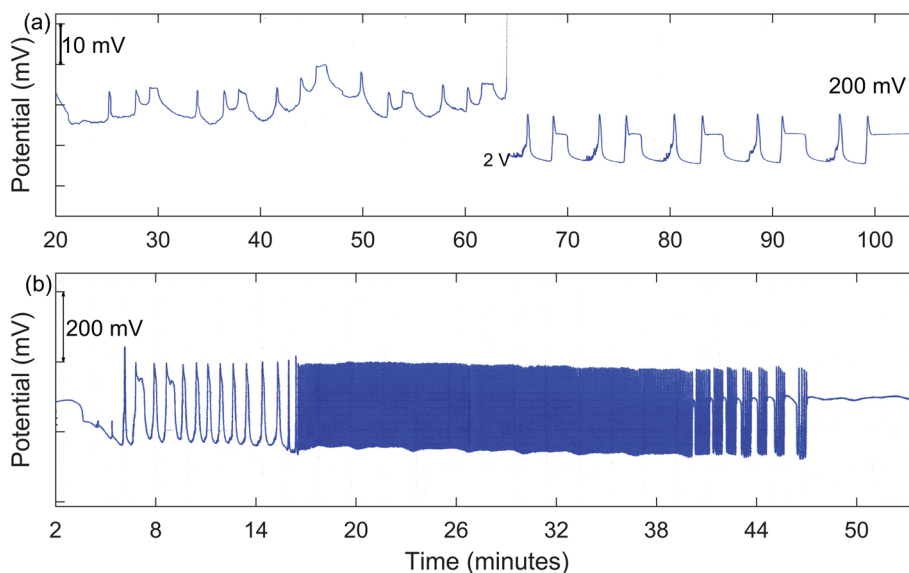


**Fig. 3** Measured Pt potential for the BZ-MeMA system in batch at 25 °C: (a) birhythmicity and mixed mode oscillations  $[3^1_5(2^1_4)2^0]$ . During transition from lower to higher state, potential full-scale setting was changed from 100 mV to 2 V.  $[\text{NaBrO}_3]_0 = 1.60 \text{ M}$ ;  $[\text{MeMA}]_0 = 0.500 \text{ M}$ ;  $[\text{NaBr}]_0 = 0.160 \text{ M}$ ;  $[\text{MnSO}_4]_0 = 0.0100 \text{ M}$ ;  $[\text{H}_2\text{SO}_4]_0 = 0.0188 \text{ M}$ . Stirring rate, 326 rpm; (b) mixed mode oscillations  $[(2^1_2)]$ , simple periodic oscillations ( $9^0$ ), quasiperiodicity, and bursting oscillations  $[(6^1_2)(5^1_3)4^0]$ .  $[\text{NaBrO}_3]_0 = 2.00 \text{ M}$ ;  $[\text{MeMA}]_0 = 1.600 \text{ M}$ ;  $[\text{NaBr}]_0 = 0.200 \text{ M}$ ;  $[\text{MnSO}_4]_0 = 0.0150 \text{ M}$ ;  $[\text{H}_2\text{SO}_4]_0 = 0.0100 \text{ M}$ . Stirring rate, 635 rpm.

**Table 4** Model for BZ batch oscillator with MeMA

#### Minimal bromate subsystem

- (1)  $\text{BrO}_3^- + \text{Br}^- + 2\text{H}^+ \leftrightarrow \text{HBrO}_2 + \text{HOBr}$
- (2)  $\text{HBrO}_2 + \text{Br}^- + \text{H}^+ \leftrightarrow 2\text{HOBr}$
- (3)  $\text{HOBr} + \text{Br}^- + \text{H}^+ \leftrightarrow \text{Br}_2 + \text{H}_2\text{O}$
- (4)  $\text{BrO}_3^- + \text{HBrO}_2 + \text{H}^+ \leftrightarrow 2\text{BrO}_2 + \text{H}_2\text{O}$
- (5)  $\text{Mn}^{2+} + \text{BrO}_2 + \text{H}^+ \leftrightarrow \text{Mn}^{3+} + \text{HBrO}_2$
- (6)  $\text{Mn}^{3+} + \text{BrO}_2 + \text{H}_2\text{O} \leftrightarrow \text{Mn}^{2+} + \text{BrO}_3^- + 2\text{H}^+$
- (7)  $2\text{HBrO}_2 \leftrightarrow \text{BrO}_3^- + \text{HOBr} + \text{H}^+$

#### Bromine-methylmalonic acid subsystem

- (8)  $\text{MeMA} \leftrightarrow \text{ENOL}$
- (9)  $\text{ENOL} + \text{Br}_2 \rightarrow \text{BrMeMA} + \text{Br}^- + \text{H}^+$
- (10)  $\text{MeMA} + \text{HOBr} \rightarrow \text{BrMeMA} + \text{H}_2\text{O}$

#### Manganese-bromomethylmalonic acid subsystem

- (11)  $\text{Mn}^{3+} + \text{BrMeMA} \leftrightarrow [\text{Mn(III)BrMeMA}]^+ + 2\text{H}^+$
- (12)  $\text{Mn}^{3+} + [\text{Mn(III)BrMeMA}]^+ \rightarrow \text{MeTA} + 2\text{Mn}^{2+} + \text{Br}^- + \text{H}^+$

#### Abbreviations

MeMA  $\sim \text{CH}_3\text{CH}(\text{COOH})_2 \sim$  methylmalonic acid

ENOL  $\sim (\text{HOOC})\text{C}(\text{CH}_3) = \text{C}(\text{OH})_2$

BrMeMA  $\sim \text{CH}_3\text{BrC}(\text{COOH})_2 \sim$  bromomethylmalonic acid

MeTA  $\sim \text{CH}_3\text{COH}(\text{COOH})_2 \sim$  methyltartronic acid

$$\begin{aligned}
 k_1 &= 2.1 \text{ M}^{-3} \text{ s}^{-1}; k_{-1} = 1 \times 10^4 \text{ M}^{-1} \text{ s}^{-1} \\
 k_2 &= 2 \times 10^9 \text{ M}^{-2} \text{ s}^{-1}; k_{-2} = 5.0 \times 10^{-5} \text{ M}^{-1} \text{ s}^{-1} \\
 k_3 &= 8 \times 10^9 \text{ M}^{-2} \text{ s}^{-1}; k_{-3} = 110 \text{ s}^{-1} \\
 k_4 &= 1 \times 10^4 \text{ M}^{-2} \text{ s}^{-1}; k_{-4} = 2.0 \times 10^7 \text{ M}^{-1} \text{ s}^{-1} \\
 k_5 &= 1.8 \times 10^5 \text{ M}^{-2} \text{ s}^{-1}; k_{-5} = 2.4 \times 10^7 \text{ M}^{-1} \text{ s}^{-1} \\
 k_6 &= 35 \text{ M}^{-1} \text{ s}^{-1}; k_{-6} = 1.3 \times 10^{-4} \text{ M}^{-3} \text{ s}^{-1} \\
 k_7 &= 4 \times 10^7 \text{ M}^{-1} \text{ s}^{-1}; k_{-7} = 2.1 \times 10^{-10} \text{ M}^{-2} \text{ s}^{-1} \\
 k_8 &= 4.5 \times 10^{-4} \text{ s}^{-1}; k_{-8} = 100 \text{ s}^{-1} \\
 k_9 &= 5 \times 10^4 \text{ M}^{-1} \text{ s}^{-1} \\
 k_{10} &= 80 \text{ M}^{-1} \text{ s}^{-1} \\
 k_{11} &= 5 \times 10^5 \text{ M}^{-1} \text{ s}^{-1}; k_{-11} = 1 \times 10^5 \text{ M}^{-2} \text{ s}^{-1} \\
 k_{12} &= 6 \times 10^2 \text{ M}^{-1} \text{ s}^{-1}
 \end{aligned}$$

manganese-bromomethylmalonic acid subsystem which features the reversible formation of a manganese(III) complex with BrMeMA, followed by two-electron oxidation to methyltartronic acid (MeTA) and  $\text{Mn}^{2+}$ . The fact that the solution color turns brown during the formation of a peak similarly to what was observed in the BZ reaction with MA lends support to the role of  $[\text{Mn(III)BrMeMA}]^+$ . For a typical run not showing birhythmicity, one can generally identify four rather distinct regions leading up to the appearance of oscillations. The reaction of  $\text{BrO}_3^-$  with  $\text{Br}^-$  and  $\text{H}^+$  in step 1 of the proposed model

takes place very rapidly, as evidenced by the nearly immediate appearance of a reddish-orange color apparently due to  $\text{Br}_2$  formation. Simultaneously, a very large increase in potential occurs. This is followed by a much slower reaction involving the reversible conversion of MeMA to the enol form (step 8). During this process a more gradual increase in potential takes place and generally a “cap” is formed. As this is occurring, the orange color turns yellow orange, indicating partial reaction of the newly formed enol with  $\text{Br}_2$ . The next phase of the reaction corresponds to the somewhat faster reaction of enol with  $\text{Br}_2$  to

Table 5 Rate constant values for enolization of MeMA

$k_8$ (s <sup>-1</sup> )	Ref.
$1.63 \times 10^{-4}$	13
$5.56 \times 10^{-5}$	12
$5.7 \times 10^{-5}$	14
$4.87 \times 10^{-5}$	9
$5.2 \times 10^{-5}$	15
$3.96 \times 10^{-4}$	16
$4.4 \times 10^{-4}$	17

form BrMeMA in step 9 of the model. There is a noticeable drop in potential during this step and the solution becomes yellow. Finally, there is another rather slow process (step 11) which is thought to be the reversible reaction of  $\text{Mn}^{3+}$  with BrMeMA to form the  $[\text{Mn(III)BrMeMA}]^+$  complex. During this step, the potential drops further and the solution becomes light yellow. Eventually, oscillations begin, as indicated both by the increase in potential and the appearance of the brown color of the complex. During oscillations, the solution color then oscillates between amber and brown, likely due to the equilibrium between  $\text{Mn}^{3+}$  and  $[\text{Mn(III)BrMeMA}]^+$  in step 11. Finally, oscillations stop when  $[\text{Mn(III)BrMeMA}]^+$  is sufficiently depleted by conversion to MeTA and  $\text{Mn}^{2+}$  in step 12.

Computer simulations based on the model in Table 4 were carried out with Berkeley Madonna software using the Rosenbrock method for integrating stiff differential equations. The rate constants used for the minimal bromate subsystem are based on previously published values.<sup>11</sup> Over many years, the kinetics of the enolization of MeMA as in step (8) has been studied by several investigators, including Furrow,<sup>13</sup> Ruoff *et al.*,<sup>9,12,14,15</sup> Williams and Graham,<sup>16</sup> and Yoshimoto *et al.*<sup>17</sup> Their results as summarized in Table 5 reflect a disparity of

nearly an order of magnitude in  $k_8$ . Data from the latter two references mentioned above allow an estimate of the value of  $k_{-8}$  for the reverse of the enolization reaction, but they do not agree. However, there is agreement that  $k_{-8} \gg k_8$ .

The rate constant values for reactions in the bromine-methylmalonic acid and manganese-bromomethylmalonic acid subsystems were obtained by treating them as variable parameters in computer simulations using the model in Table 4.

Before attempting to reproduce the complex oscillations obtained in most of the experiments, we first tried to simulate the simpler periodic oscillations observed using lower concentrations of reactants as in Fig. 1(a). To determine the importance of  $[\text{Mn(III)BrMeMA}]^+$ , simulations were attempted without including the manganese-bromomethylmalonic acid subsystem (*i.e.*, letting  $k_{11} = k_{-11} = k_{12} = 0$ ). Interestingly, it was not possible to produce oscillations under these conditions.

Once it was determined the manganese-bromomethylmalonic acid subsystem needed to be part of the model, it was found that the set of rate constants giving the best fit under the experimental conditions for Fig. 1(a) was:  $k_8 = 4.5 \times 10^{-4} \text{ s}^{-1}$ ;  $k_{-8} = 100 \text{ s}^{-1}$ ;  $k_9 = 5 \times 10^4 \text{ M}^{-1} \text{ s}^{-1}$ ;  $k_{10} = 80 \text{ M}^{-1} \text{ s}^{-1}$ ;  $k_{11} = 5 \times 10^5 \text{ M}^{-1} \text{ s}^{-1}$ ;  $k_{-11} = 1 \times 10^5 \text{ M}^{-2} \text{ s}^{-1}$ ;  $k_{12} = 600 \text{ M}^{-1} \text{ s}^{-1}$ . The calculated oscillations under these conditions are shown in Fig. 4(a). Note that these oscillations give good agreement with experiment in terms of the induction period, period of oscillations, and total number of peaks observed. Also, as the period increases toward the latter part of the experiment, the peaks begin to show a broadening or formation of a “shoulder,” as observed experimentally. This is especially evident in Fig. 4(b) where a  $k_{10}$  value of  $40 \text{ M}^{-1} \text{ s}^{-1}$  is used in the plot of  $[\text{BrO}_2]$  and  $[\text{HBrO}_2]$  vs. time. This suggests that the intermediates,  $\text{BrO}_2$  and  $\text{HBrO}_2$ , may play a significant role in determining the shape of the oscillatory peaks.

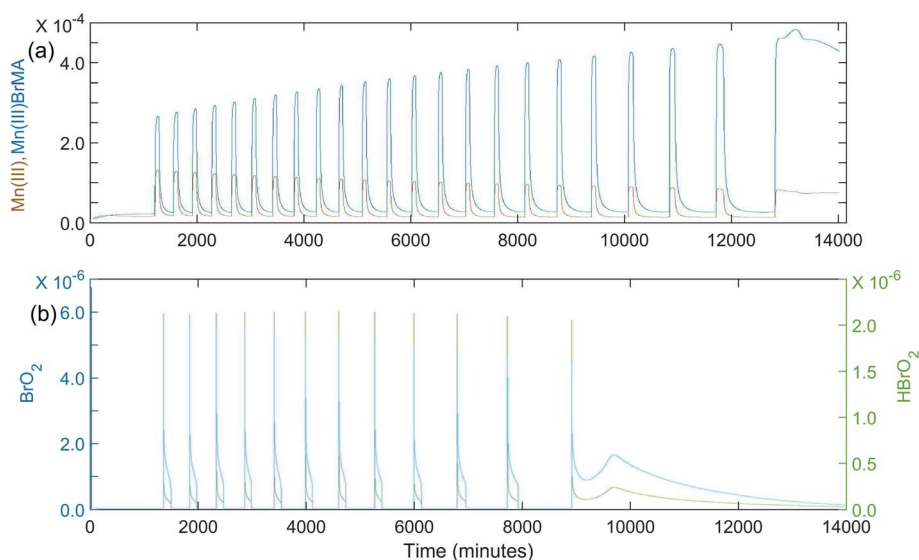


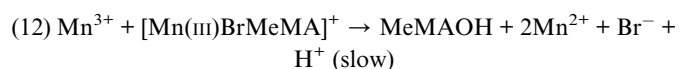
Fig. 4 Calculated oscillations for the BZ-MeMA system in batch at 25 °C.  $[\text{NaBrO}_3]_0 = 0.200 \text{ M}$ ;  $[\text{MeMA}]_0 = 0.120 \text{ M}$ ;  $[\text{NaBr}]_0 = 0.0200 \text{ M}$ ;  $[\text{MnSO}_4]_0 = 0.00600 \text{ M}$ ;  $[\text{H}^+]_0 = 0.300 \text{ M}$ . Time axis units are seconds: (a)  $[\text{Mn}^{3+}]_0$  (brown) and  $[\text{Mn(III)BrMeMA}]_0$  (blue) using rate constants given in Table 4; (b)  $[\text{BrO}_2]_0$  (blue) and  $[\text{HBrO}_2]_0$  (green) using rate constants given in Table 4 except  $k_{10} = 40 \text{ M}^{-1} \text{ s}^{-1}$ .



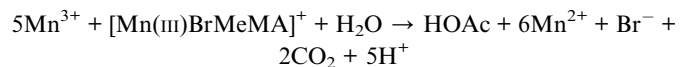
Although some of the rate constant values were treated as adjustable parameters in the simulations, nearly all of these values seem quite reasonable. For example, both the enolization rate and the rate of reaction of Br<sub>2</sub> with MeMA have been shown experimentally to be significantly lower than for comparable reactions with MA. This is reflected in the smaller rate constant values used for steps (8) and (9) with MeMA. The only adjustable rate constant used in the simulations with a value larger than that for a similar reaction with MA is  $k_{10}$ , the rate constant for reaction of MeMA with HOBr. While oscillations can be obtained with a  $k_{10}$  value comparable to that for reaction with MA ( $8.2 \text{ M}^{-1} \text{ s}^{-1}$ ), a significantly larger value is required to give the proper number of peaks with MeMA. Simulations show that, the larger the value of  $k_{10}$ , the greater the number of oscillations formed. Also, the period of oscillations depends greatly on  $k_{12}$ —the larger its value, the shorter the period. This seems reasonable, considering that  $k_{12}$  corresponds to the last step in the manganese–bromomethylmalonic acid subsystem.

Attempts to simulate the complex oscillations observed in this study, such as in Fig. 1(b) and 2, were unsuccessful. However, by using  $[\text{H}^+]_0$  values larger than those used in our experiments (e.g., 0.25–0.50 M) simple periodic oscillations could be obtained. This suggests that the model in Table 4 is not complete and that one or more steps producing  $\text{H}^+$  may be required in order to simulate the complex oscillations.

Ruoff *et al.*<sup>18,19</sup> have studied the oxidation of MeMA by cerium(IV) and found that in this case about 70–80% of MeMA reacts rapidly to form acetic acid (HOAc) and CO<sub>2</sub>. Their proposed scheme suggests the oxidation of MeMA to MeMAOH at a moderate rate followed by the rapid conversion of MeMAOH to pyruvic acid (Pyr). Finally, Pyr is converted rapidly to HOAc. Assuming the same principal oxidation products are formed with the Mn(II)-catalyzed system, it would seem reasonable to add steps (13) and (14) to the manganese–bromomalononic acid subsystem, thus giving:

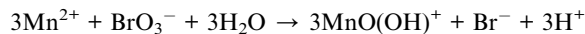


The sum of steps (12), (13), and (14) would give an overall stoichiometry of:

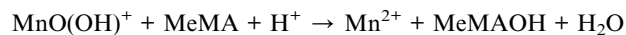


However, using reasonable values for  $k_{12}$ ,  $k_{13}$ , and  $k_{14}$  gave simulations very similar to those obtained without including steps (13) and (14).

Another possible reaction that could produce additional  $\text{H}^+$  is one suggested by Hanazaki *et al.*<sup>20</sup> to partially account for pH oscillations with the bromate-sulfite system in a CSTR:



This reaction is thought to involve autocatalytic production of  $\text{MnO(OH)}^+$  with  $\text{Mn(OH)}^{2+}$  as an intermediate. Including the above reaction in our model again gave simulations similar to those obtained previously. If  $\text{MnO(OH)}^+$  were to play a significant role in the model, it possibly could oxidize MeMA according to the reaction:



However, the addition of this reaction likewise has no effect on the simulations. Apparently,  $\text{MnO(OH)}^+$  is not present to a sufficient extent in the present system which typically is in a pH range of 1–2.

## Conclusions

We have obtained both periodic and complex oscillations in the potential of a Pt electrode in batch with the Mn(II)-catalyzed BZ reaction involving MeMA. Types of complex behavior observed include mixed mode oscillations (MMO), birhythmicity (BI), bursting (BR), quasiperiodicity (Q), and possible chaotic oscillations. Complex oscillations occurred only with rather high initial concentrations of NaBrO<sub>3</sub> and MeMA. Systematic variations in the temperature, stirring rate, initial bromate/methylmalonic acid ratio, and initial concentrations of bromide, Mn(II), and acid or base allowed us to elucidate oscillation patterns with respect to the reaction conditions. The  $[\text{NaBrO}_3]_0/[\text{MeMA}]_0$  ratio is the main factor determining whether complex oscillations are obtained, and of what type. Other factors found to affect the specific type of oscillations observed were temperature,  $[\text{NaBr}]_0$ ,  $[\text{MnSO}_4]_0$ ,  $[\text{H}_2\text{SO}_4]_0$  or  $[\text{NaOH}]_0$ , and stirring rate.

This is the first report of complex oscillations in the BZ reaction with MeMA in a stirred system. Because of the simplicity of the experimental procedure, the batch system lends itself to use in teaching laboratories. The procedure only involves dissolving three solid reagents in water (and possibly either H<sub>2</sub>SO<sub>4</sub> or NaOH). Depending on conditions, various types of complex oscillations in potential and absorbance can be observed.

A model very similar to that for the Mn(II)-catalyzed BZ reaction with MA has been proposed for the present system. The minimal bromate subsystem is the same as with other Mn(II)-catalyzed BZ reactions. The bromine–methylmalonic acid subsystem involves previously reported reactions that parallel those with MA. A critical part of the mechanism involves the reversible formation of a manganese(III) complex with BrMeMA, followed by two-electron oxidation to MeTA and Mn<sup>2+</sup>. In addition to the appearance of a brown color during oscillations, strong evidence for including the manganese–bromomethylmalonic acid subsystem is that periodic oscillations could be obtained by computer simulation only if  $[\text{Mn(III)BrMeMA}]^+$  is included in the mechanism. (This suggests that the Mn(III)



complex may be formed in all Mn(II)-catalyzed BZ reactions with MA or MeMA, but in some cases may not be present at a high enough concentration that it can be detected.) Although simulation of periodic oscillations with the proposed model was successful, this was not the case for complex oscillations. It is suggested that one or more steps involving formation of  $H^+$  may need to be added to the model in order to simulate complex oscillations. This could involve formation of further oxidation products, such as Pyr and/or HOAc.

It is interesting that bursting behavior similar to that described above was originally reported for biological systems. For example, bursting due to a changing membrane potential is common in various types of neurons, including pacemaker neurons. The latter have been shown to control rhythmic tasks such as breathing, locomotion, eating, and sleeping.<sup>21</sup> Bursting also has been studied in various electrochemical systems, including  $H_2O_2$  reduction on platinum, iron dissolution in sulfuric acid with halogen additives, and with dichromate ions coupled with graphite or zinc electrodes.<sup>22</sup> In addition, the chlorine dioxide-iodide reaction in a system consisting of two coupled CSTRs (continuous-flow stir tank reactors) has been found to give neuron-like bursting behavior.<sup>23</sup> The insight into the mechanisms that generate the observed oscillation patterns in the present work possibly could elucidate processes that lead to similar oscillation patterns in biological systems and other natural phenomena.

It is our hope that this study of the Mn(II)-catalyzed BZ reaction using MeMA as the organic substrate presents new investigation opportunities in nonlinear chemical systems. For example, it would be informative to study this reaction in a flow system, especially to observe how the specific type of complex oscillations might vary with the reciprocal residence time  $k_0$ .

## Conflicts of interest

There are no conflicts of interest to declare.

## Acknowledgements

We gratefully acknowledge the support of Westminster College in this research.

## References

- 1 R. J. Field, E. Koros and R. M. Noyes, *J. Am. Chem. Soc.*, 1972, **94**, 8649–8664.
- 2 P. Ruoff, *J. Phys. Chem.*, 1992, **96**, 9104–9106.
- 3 J. Wang, P. G. Sorensen and F. Hynne, *J. Phys. Chem.*, 1994, **98**, 725–727.
- 4 P. E. Strizhak and A. L. Kawczynski, *J. Phys. Chem.*, 1995, **99**, 10830–10833.
- 5 M. Rachwalska and A. L. Kawczynski, *J. Phys. Chem. A*, 1997, **101**, 1518–1522.
- 6 B. R. Johnson, S. K. Scott and B. W. Thompson, *Chaos*, 1997, **7**, 350–358.
- 7 Lj. Kolar-Anic, S. M. Blagojevic, N. Pejic, N. Begovic, S. N. Blagojevic and S. J. Anic, *J. Serb. Chem. Soc.*, 2006, **71**, 605–612.
- 8 S. M. Blagojevic, S. R. Anic, Z. D. Cupic, S. N. Blagojevic and Lj. Z. Kolar-Anic, *Russ. J. Phys. Chem. A*, 2013, **87**, 2140–2145.
- 9 E. W. Hansen and P. Ruoff, *J. Phys. Chem.*, 1989, **93**, 264–269.
- 10 S. S. Sun, H.-P. Lin, Y.-F. Chen and J.-J. Jwo, *J. Chin. Biochem. Soc.*, 1994, **41**, 651–658.
- 11 G. A. Frerichs, J. Jones, X. Huang, M. Gebrekidan, J. Burch and M. Y. Cheng, *J. Phys. Chem. A*, 2019, **123**, 1303–1310.
- 12 P. Ruoff and B. Z. Schwitters, *Z. Phys. Chem. Neue Folge*, 1983, **135**, 171–184.
- 13 S. D. Furrow, *Int. J. Chem. Kinet.*, 1979, **11**, 131–145.
- 14 E. W. Hansen and P. Ruoff, *J. Phys. Chem.*, 1988, **92**, 2641–2645.
- 15 E. W. Hansen and P. Ruoff, *J. Phys. Chem.*, 1989, **93**, 2696–2704.
- 16 D. L. H. Williams and A. Graham, *Tetrahedron*, 1992, **48**, 7973–7978.
- 17 M. Yoshimoto, T. Matsunaga, M. Tanaka and S. Kurosawa, *Anal. Chem. Res.*, 2016, **8**, 9–15.
- 18 P. Ruoff and G. Nevdal, *J. Phys. Chem.*, 1989, **93**, 7802–7806.
- 19 P. O. Kvernberg, E. W. Hansen, B. Pedersen, A. Rasmussen and P. Ruoff, *J. Phys. Chem.*, 1997, **101**, 2327–2331.
- 20 N. Okasaki, G. Rabai and I. Hanazaki, *J. Phys. Chem.*, 1999, **103**, 10915–10920.
- 21 J.-M. Ramirez, H. Koch, A. J. Garcia, III, A. Doi and S. Zanella, *J. Biol. Phys.*, 2011, **37**, 241–261.
- 22 I. Z. Kiss, Lv. Qing, L. Organ and J. L. Hudson, *PCCP Phys. Chem. Chem. Phys.*, 2006, **8**, 2707–2715.
- 23 M. Dolnik and I. R. Epstein, *J. Chem. Phys.*, 1993, **2**, 1149–1155.

